

**NASA TECHNICAL  
MEMORANDUM**



**NASA TM X-2994**

**NASA TM X-2994**

**CASE FILE  
COPY**

**ELECTRICAL HEATING TESTS OF  
URANIUM DIOXIDE EXTERNAL FUEL  
CONFIGURATION AT EMITTER  
TEMPERATURE OF 1900 K**

*by Dominic C. Dilanni and John T. Mayer*

*Lewis Research Center*

*Cleveland, Ohio 44135*

1. Report No. <b>NASA TM X-2994</b>	2. Government Accession No.	3. Recipient's Catalog No.	
4. Title and Subtitle <b>ELECTRICAL HEATING TESTS OF URANIUM DIOXIDE EXTERNAL FUEL CONFIGURATION AT EMITTER TEMPERATURE OF 1900 K</b>		5. Report Date <b>MARCH 1974</b>	
		6. Performing Organization Code	
7. Author(s) <b>Dominic C. DiIanni and John T. Mayer</b>		8. Performing Organization Report No. <b>E-7554</b>	
		10. Work Unit No. <b>503-25</b>	
9. Performing Organization Name and Address <b>Lewis Research Center National Aeronautics and Space Administration Cleveland, Ohio 44135</b>		11. Contract or Grant No.	
		13. Type of Report and Period Covered <b>Technical Memorandum</b>	
12. Sponsoring Agency Name and Address <b>National Aeronautics and Space Administration Washington, D. C. 20546</b>		14. Sponsoring Agency Code	
		15. Supplementary Notes	
16. Abstract <p>Testing of two fuel clad specimens for thermionic reactor application is described. The annular <math>UO_2</math> fuel was clad on both sides with tungsten; heat rejection was radially inward. The tests were intended to study inner clad stability, fuel redistribution, and fuel melting problems. The specimens were tested in a vacuum chamber using electron bombardment heating. Fuel structural changes were studied using periodic gammagraphs and posttest metallography. The first specimen test was terminated at 50 hours because of a braze failure. The second specimen was tested for 240 hours when an outer clad leak developed due to a tungsten-water reaction. The fuel developed numerous cracks on cooldown but the inner clad remained dimensionally stable. The fuel cover gas did not impede the rate of fuel redistribution. Posttest examination showed the fuel had not melted during operation.</p>			
17. Key Words (Suggested by Author(s)) <b>Uranium dioxide; External fuel configuration; Tungsten; Thermionics; Electric heating (electron bombardment); Nuclear fuel</b>		18. Distribution Statement <b>Unclassified - unlimited</b>	
19. Security Classif. (of this report) <b>Unclassified</b>		20. Security Classif. (of this page) <b>Unclassified</b>	21. No. of Pages <b>28</b>
		22. Price* <b>\$3.00</b>	
Cat. 22			

\* For sale by the National Technical Information Service, Springfield, Virginia 22151

# ELECTRICAL HEATING TESTS OF URANIUM DIOXIDE EXTERNAL FUEL CONFIGURATION AT EMITTER TEMPERATURE OF 1900 K

by Dominic C. DiIanni and John T. Mayer

Lewis Research Center

## SUMMARY

An externally fueled configuration for thermionic application was tested using uranium dioxide ( $\text{UO}_2$ ) clad with tungsten operating at 1900 K. Evaluated were: (1) possible fuel melting during startup, (2) compressive stresses on the emitter during shutdown after fuel redistribution, and (3) effect of cover gas on fuel redistribution. To investigate these problems, a test program was initiated using  $\text{UO}_2$ -fueled tungsten clad specimens. The testing was done in a vacuum furnace using electron bombardment to heat the specimens. Periodic gammagraphs of the specimens were taken, and post-test metallography was performed.

The first specimen was tested for 50 hours at a maximum outer clad temperature of 2450 K and underwent one thermal cycle. A second specimen was tested for 240 hours at an outer clad temperature of 2550 K and underwent five thermal cycles. The inner clad temperature for both specimens ranged from 1800 to 2050 K.

The second specimen showed various degrees of fuel restructuring during the test and some evidence of crack healing. Although there was no dimensional change to the inner clad, the outer clad reacted with water vapor inside the fuel area. This resulted in a leak which caused the termination of the test.

The first specimen showed that fuel redistribution had started and radial cracks developed because of cooldown. The fuel of the second specimen had undergone gross redistribution, and densification was in progress. Posttest metallography showed fuel melting had not occurred during operation and fuel radial cracks occurred on cooldown.

## INTRODUCTION

Thermionic reactors are candidates for the power supply or for electric propulsion of space vehicles. One of the concepts studied employs an external fuel configuration.

In this configuration the emitter surface is at the inner diameter of the fuel pin where heat removal occurs. The fuel ( $\text{UO}_2$ ) may be annularly configured (ref. 1) or segmenting webs may be used (ref. 2) to reduce the temperature difference across the fuel and to facilitate fuel breakup. The fuel volume fraction is, of course, less when webs or a revolver concept (ref. 3) is used.

In the revolver concept a tungsten cylindrical body would contain the  $\text{UO}_2$  fuel in six peripheral holes. The tungsten body would be in tension due to fuel swelling. An opposite condition would exist in the external fuel configuration (ref. 1).

A possible problem with the externally fueled configuration with the fuel in the shape of a hollow cylinder clad on both the inside and outside diameter is related to the greater thermal expansion of  $\text{UO}_2$  as compared to tungsten (ref. 1). This thermal expansion difference, for a typical situation where the  $\text{UO}_2$  had redeposited on the emitter, could cause high compressive stresses during cooldown and result in the deformation or collapse of the emitter. Furthermore during heatup the fuel expands more than the tungsten, a fuel-emitter gap will be created that may lead to fuel melting before fuel redistribution can occur (ref. 4). A method of avoiding fuel melting would be to introduce a cover gas (He) over the fuel. Whether a cover gas at a pressure adequate for heat transfer would seriously impede the rate of fuel redistribution is unknown.

This report describes two tests of a test program to examine these problems for an externally configured fuel specimen concept using nonsegmented fuel. The two fuel specimens were heated by an electron bombardment heater in a vacuum chamber. Heat was removed at the center of the fuel annulus. The fuel specimen was thermal cycled during and after fuel redistribution. The outer and inner tungsten clad were tested at 2550 and 1900 K, respectively. This was followed by a posttest examination of the fuel specimen.

## TEST SPECIMEN

The specimen (fig. 1) was one of a series proposed for an out-of-pile test program. Specimens were to have varying inner clad and  $\text{UO}_2$  thicknesses to determine the degree of dimensional stability of the inner clad. Two specimens were run in this experiment, each with a constant clad thickness of 1.52 millimeters (0.060 in.). The length of each specimen was approximately 3.81 centimeters (1.5 in.). The  $\text{UO}_2$  thicknesses were 3.18 millimeters (0.125 in.) for specimen 1 and 4.57 millimeters (0.180 in.) for specimen 2. The smaller fuel thickness was based on criticality calculations from reference 1. The fuel volume fraction and the maximum fuel temperature of 2420 to 2570 K (to achieve fuel redistribution in a reasonable time) were also factors in selecting the fuel and clad thicknesses. The outer clad was designed to contain a cover gas over the

fuel and to prevent  $\text{UO}_2$  loss. An outer clad thickness of 2.03 millimeters (0.080 in.) was selected for containing thermocouples, which supplemented the optical temperature measurements. An inner clad temperature of 1870 to 1970 K was selected as appropriate for reasonable thermionic conversion efficiencies.

Descriptions of various aspects of the test specimen design appear in the following sections.

### Materials

The inner and outer clad were prepared from wrought tungsten rod having 140 ppm of metallic impurities and an oxygen content of 570 ppm. Tungsten surfaces were free from cracks, voids, pits or deep scratches under a  $\times 10$  visual magnification and dye penetrant inspection.

Natural  $\text{UO}_2$  powder was isostatically pressed and sintered to 93.6 percent of theoretical density. The oxygen to uranium ratio was 2.00 to 2.01. Figure 2 shows the as-received  $\text{UO}_2$  microstructure at  $\times 12$  both etched and unetched. Analysis showed that the total metallic impurities in the fuel were less than 115 ppm, of which 75 ppm were aluminum, iron, chromium, and nickel.

### Heat Dams

Figure 1 shows the heat dams at the ends of the specimen. These dams were designed to reduce the axial heat loss. The criterion was 700 K  $\Delta T$  radially across a 4.57-millimeter (0.180-in.) thick  $\text{UO}_2$  fuel annulus with the inner clad at 1875 K. The heat dam geometry shown on figure 1 evolved from the heat-transfer analysis (STHTP) (ref. 5) with a 42-percent helium and 58-percent argon binary gas in the gap formed between the heat sink and the test specimen inside clad. Calculations showed that with a heat flux of 104 watts per square centimeter on the outside clad surface, 62 percent of the heat would be transferred radially through the fuel.

### Cover Gas

Helium cover gas was introduced to improve fuel-to-clad heat transfer. An operating pressure of 0.03 to 0.04 newtons per square centimeter (2 to 3 torr) was selected after considering the gas thermal conductivity and impediment to  $\text{UO}_2$  redistribution across the gap. (Gluyas (ref. 6) showed that the presence of argon at  $10 \text{ N/cm}^2$  (1 atm)

could reduce the rate of mass transfer of  $\text{UO}_2$  by an order of magnitude. Whether such a reduction applies to helium at 0.03 to 0.04  $\text{N/cm}^2$  is questionable.)

### Binary Gas

Heat leaving the specimen was transferred across a static helium and argon gas annulus to the heat sink (water flow channel) located in the center of the specimen (see fig. 1). The inner clad temperature was adjusted by changing the gas composition in the 0.63-millimeter (0.025-in.) annulus. When the composition was changed from 100 percent helium to 100 percent argon (at design inner clad temperature of 1875 K), a 400 K variation in inner clad temperature could be achieved (at constant power).

### Fuel and Clad Radial Dimensions

Table I shows the as-built dimensions for both specimens and the design operating temperature dimensions for specimen 2. The design temperature values were calculated from the coefficient of thermal expansion curves for tungsten and  $\text{UO}_2$  given in references 7 and 8. The high temperature inside and outside gaps were calculated assuming the  $\text{UO}_2$  to be in the form of a hollow cylinder. However, for expansion and assembly purposes the fuel cylinder was split axially into two half cylinders. The splits created two 0.85-millimeter (0.030-in.) gaps on the circumference, permitting fuel movement within the inside and outside clad. The actual spacing between the fuel and clad was not known. However, the heat-transfer analysis showed the fuel would not melt when the maximum spacing existed between the fuel and the inner clad (a worst case condition).

### Braze Areas Joining Tungsten Through a Transition to

### Stainless-Steel Tubing

The tungsten tubing at the top end of the test specimen was joined to the molybdenum tube with an 82-percent gold - 18-percent nickel, 1250 K braze. The tungsten tubing at the bottom end of the test specimen was joined to a molybdenum tube with Palniro No. 4 Braze (30-percent Au - 34-percent Pd - 36-percent Ni). The molybdenum tubing was then brazed to a 304 stainless steel tube using an 82-percent gold - 18-percent nickel braze metal.

## TEST FACILITY

The specimen was tested in a high-vacuum chamber using electron-bombardment (EB) heating. This furnace, along with its associated fluid and electrical systems, is described in the following sections.

### Electron-Bombardment Heater and Power Supply

Figure 3 shows the specimen and the EB filament, which is a two-turn coil of 1.52-millimeter (0.060-in.) diameter tungsten. The filament connections to the power supply are also shown in the figure. The 60 hertz, alternating current (ac) portion of the supply is used for resistive heating of the filament. When the filament is hot enough, the electrons coming off the filament through thermionic emission are repulsed by the large negative direct current (dc) voltage of the filament. These electrons then bombard the specimen, which is grounded.

The power supply is capable of providing 100 amperes at 50 volts ac for heating the filament. At normal operating conditions 78 amperes at 13 volts is sufficient to give a filament temperature of about 2400 K. The direct current accelerating circuit has a capability of 5 amperes at 2500 volts, but it is normally operated at 1000 volts. This gives an accelerating current of about 3 amperes.

The specimen and filament are surrounded by a three-element tantalum radiation shield. This shield is insulated electrically from the chamber through the use of alumina sleeves. A slit in the front of the shield allows pyrometer sighting of the specimen and filament. Also shown in the figure is a copper cooling jacket attached to the specimen. This is required to keep the lower braze area temperature below 1250 K. The water lines for this jacket, as well as thermocouple leads from the outside of the specimen, are brought out through fittings in the lower flange of the chamber.

### Vacuum Chamber

The test chamber (fig. 4) is a stainless-steel tank with copper water-cooling lines brazed to the outside. It is attached to a liquid-nitrogen-trapped diffusion pump at the vacuum manifold. A standard ionization gage measures the chamber pressure. Typical pressure obtainable is  $2.7 \times 10^{-8}$  newton per square centimeter ( $2 \times 10^{-6}$  torr) at operating temperature. An additional ion gage is mounted near the cold trap in the vacuum system.

## Gas System

A schematic of the piping to supply helium and argon to the specimen is shown in figure 5. The gas system includes (1) a mixing tank with a pressure gage for providing variable helium-argon mixtures to the specimen binary gas gap, (2) piping to provide low-pressure helium to the  $\text{UO}_2$  cover gas volume, (3) provision for low-pressure helium purging of the chamber vacuum system, and (4) connection to the chamber vent valve so that the chamber vacuum system could be used to out-gas and leak-check the gas system piping.

Normal operating pressures for the two gas volumes are 12 newtons per square centimeter (3 psig) for the helium-argon mixture and 0.027 newtons per square centimeter (2 torr) for the cover gas. Pressure switches are connected to each gas volume. An alarm is given for a drop in helium-argon pressure or a rise in cover gas pressure.

## Instrumentation

Tungsten - 3-percent rhenium/tungsten - 25-percent rhenium thermocouples were used to measure clad temperature. However, the outer clad and top inner clad thermocouples were inaccurate and are not reported. The four thermocouples at the bottom end of the inner clad were continuously recorded. In addition, optical pyrometer readings of the outer clad temperature were taken at regular intervals. Other readings taken during the test included chamber vacuum, power supply characteristics, gas pressures, and filament temperature.

## TEST PROCEDURES AND OPERATIONS

The general test plan can best be described as long-term thermal cycling. For each cycle the specimen was to be brought up to temperature, held there for approximately 50 hours to allow some redistribution and/or crack healing, and then returned to room temperature. Complete redistribution time for the test conditions was thought to be of the order of 200 hours. One of the purposes of the first series of thermal cycles was to get information on this process through gammagraphs.

Normal pretest procedures included (1) overnight pumping of the chamber, cover gas, and binary gas volume, (2) filling the cover gas and binary gas volumes and checking for leaks, and (3) checking out and calibrating the instrumentation. Heatup and cool-down were done at a slow rate, usually 80 K per hour, between room temperature and 875 K and at 400 K per hour above that temperature. During steady-state operation, the



heat input was adjusted for constant outer clad temperature (middle blackbody hole).

Specimen 1 operated at temperature for only 50 hours because of a failure at the bottom of the molybdenum-tungsten braze, which leaked helium and argon from the specimen into the vacuum chamber. Attempts at repair were unsuccessful so the specimen was removed. Specimen 2 operated for 240 hours at temperature. Testing was discontinued when a leak was discovered at one of the blackbody holes. The hole allowed helium cover gas to escape into the chamber.

### Specimen 1

Some difficulty was encountered in bringing specimen 1 to temperature. Periodic arcing of the high voltage components to ground, accompanied by current surges or short-term chamber vacuum spikes, caused the difficulty. These arcs would cause shutdown of the EB power supply. After correcting this problem by modifying the tantalum radiation shields, the specimen was brought up to the desired temperature and held for 50 hours without any arcing. The operating history during this period is shown in figure 6. The inset sketch shows the inner clad thermocouple locations and the direction of filament shift during the test. This shifting of the filament (due to high temperature) is responsible for the divergence of the three inner clad thermocouples during the test. (The fourth thermocouple never operated properly.) It is not known why the front and back thermocouples were affected so much. Judging from the difference in the thermocouples, the filament shift occurred continuously during the test. The total circumferential gradient was probably about 200 K at the inner clad near the end of the test.

After the test a gammagraph was taken which showed some fuel redistribution at the hot side of the specimen, as well as a longitudinal crack perpendicular to the axis of the fuel.

### Specimen 2

Specimen 2 was run at temperature for 240 hours with scheduled shutdowns at 50, 100, and 150 hours. Gammagraphs were taken during these shutdowns, as well as before and after the test. Six inadvertent partial shutdowns occurred during the 240-hour test. Four of these were minor, involving less than a 200 K drop in inner clad temperature before power was restored. The fifth, at 115 hours resulted in a drop of 500 K; the sixth due to a loss of coolant at 190 hours resulted in a drop of 1000 K. Because the sixth shutdown resulted in such a large temperature it was considered a full thermal cycle.

The operating parameters for the specimen 2 runs are shown in figure 7. It was noted after runs 1 and 3 that the EB filament had shifted to the left. However, the emitter temperature for these runs did not show the wide variation or divergence with time that the specimen 1 data showed. In fact, the specimen 2 inner clad temperature spreads for runs 1 and 3 were not markedly different from that of run 2 (where the filament remained in its centered position). Before the start of run 3, a less accurate pressure gage was installed in the cover gas piping. For runs 3 and 4 the cover gas pressure was held at about 0.7 newton per square centimeter (1 psia).

Gammagraphs taken at various intervals are shown in figure 8. Figure 8(a) shows that at 50 hours a significant void had formed (through  $UO_2$  redistribution) on the right side of the specimen. This may have been caused by the shifting of the filament since very little redistribution was seen on the left side or at the front or back. Short cracks were seen on both the front and side views of the specimen. By 100 hours the void area was visible at the front of the specimen, and some evidence of crack healing was seen. At 150 hours significant void was seen all around the specimen, except for the back. Also, the outer clad was noticeably thinner at the left and front of the specimen, and additional crack healing was seen. Figures 8(b) and (c) show the final gammagraphs taken at 240 hours. Although a void has finally started to form at the back of the specimen, it is still not very large. Several large cracks visible in the side view at 50 hours have completely disappeared. The data in figure 7 (note runs 3 and 4) show the  $\Delta t$  decreased at the bottom of the specimen while the heat input to the specimen was increased. This indicates the thermal conductivity increased in this part of the specimen. Such a change in thermal conductivity could be due to fuel redistribution, closing the gaps between the fuel and clad, and/or fuel plugging of the heat dam gap.

## POSTTEST EXAMINATION

This examination covered dimensional measurements, fuel and clad compatibility, and fuel movement, cracking, and redistribution. A reaction layer observed during gammagraphing between the fuel and the outside clad was also examined.

### Specimen 1

Specimen 1 was mounted in epoxy and sectioned for the purpose of studying the tungsten reaction layer. The sectioned specimen showed the beginning of fuel redistribution. Figure 9 is a  $\times 14.5$  montage of the radial face at the fuel midplane where maximum fuel redistribution occurred. The thin layer between the fuel and the outside clad

was identified as pure tungsten. This thin tungsten layer is discussed in the examination of specimen 2. The start of fuel redistribution is indicated by the fuel attached to the inner clad.

## Specimen 2

Dimensional measurements. - Measurements of the inside diameter of the inner cladding were made using both a telescoping gage and an inside micrometer having an accuracy of  $\pm 0.025$  millimeter (0.001 in.). These measurements at  $0^\circ$  and  $90^\circ$  showed no change after 240 hours of operation and five thermal cycles. The outside diameter of the outer cladding was measured using a calibrated micrometer whose accuracy was  $\pm 0.005$  millimeter (0.0002 in.), and the results are shown in table II. These measurements indicate that slight bulging occurred at the midplane of the specimen where the reaction was most severe (as seen in the gammagraphs).

Metallography. - The specimen was mounted in epoxy and sectioned transversely slightly below the middle blackbody hole (fig 10 cut 1). The top half of the specimen was machined to expose the clad failure and the fuel structure where the maximum redistribution occurred. Figure 11 is a  $\times 10$  montage of this face. White particles in the space between fuel and the outside clad were identified as pure tungsten using a scanning electron microscope (SEM) equipped with an energy dispersive X-ray analyzer. The SEM was capable of identifying elements having atomic numbers greater than 12. Since other elements were not found in this region it was concluded that tungsten was transported by a combination of high temperature and water vapor trapped in the void during assembly. It takes only a few ppm of water vapor to start a reversible reaction with tungsten at high temperature (private communication with K. Bowles and G. Watson of Lewis). Further examination showed that the fuel had not reacted with the tungsten. Figure 11 shows that the maximum heat flux and thermal gradient through the fuel occurred about  $15^\circ$  counterclockwise from the reference point. The minimum flux and thermal gradient through the fuel occurred  $180^\circ$  away from the maximum point. This is evident from the fuel redistribution pattern where the fuel moved from the highest to the lowest heat flux area. The redistributed fuel shows that the longitudinal fuel split was located  $40^\circ$  clockwise from the reference point (at the deep valley and large cracks  $180^\circ$  away). During cooldown large cracks occurred at the grain boundaries that were lines of weakness in the region of gross fuel redistribution. It is interesting to note that the fuel adhered to the inner clad even though many cracks appeared in the fuel structure upon cooldown.

A calculated maximum gap of 0.431 millimeter (0.017 in.) existed between the fuel and the clads (inner and outer) at the beginning of high-temperature operation. As oper-

ation continued fuel redistribution occurred filling the inner clad fuel gap and the splits with porous fuel. Evidence of this shows the conditions at the beginning of redistribution (fig. 9). It is possible that the fuel void density would increase with an increasing gap size. Voids coalescing in the grain boundaries would by vaporization and condensation migrate to the outer periphery of the fuel. Because the fuel vapor pressure increases with temperature, the voids accelerate as they move through the fuel thermal gradient. This explains the appearance of denser fuel in the outer area of the specimen as shown in figure 11. It appears that fuel cracking is independent of fuel densification since cracks propagated through the fuel. With inside and outside fuel temperatures of 1970 and 2550 K, respectively, the fuel redistributed within 240 hours, as borne out by the gammagraphs and the metallographic examination. Fuel densification time would be longer and is dependent upon gap size formed between the fuel and the inside clad during the initial high-temperature operating period.

Figure 12 shows the fuel-clad condition in the longitudinal face of the bottom half of the specimen. Figure 13 shows the longitudinal face of the top half of the specimen. Both cuts (figs. 12 and 13) made along the same plane exposed maximum and minimum temperature conditions as determined from examining the exposed faces from the first cut. The areas C and E of figures 12 and 13 show the fuel structure that operated at a higher thermal gradient than the structure shown in areas B and D. This condition is verified by comparing the shape of the fuel surface, the fuel dendritic structure, and temperature readings taken during operation. The gaps adjacent to the heat dams appear to be plugging up with fuel. More fuel has gathered in the heat dams shown in areas C and E than in B and D. As expected, the amount of fuel entering these dams is dependent on temperature. The heat dams shown in areas C and E operated at a higher temperature than those shown in areas B and D. It is reasonable to assume that these dams would be filled with fuel when fuel redistribution is complete.

## DISCUSSION OF RESULTS

The testing of these specimens was part of a larger program for studying the externally configured fuel. But further work in this area was discontinued because of the termination of the thermionic nuclear work by NASA.

### Dimensional Stability

The inside clad measurement of specimen 2 showed the inside diameter had not changed after operating at temperature for 240 hours and five thermal cycles. It is not

known whether clad stability would be maintained with continued operation. It appeared that the concentricity of the inside clad of the second specimen had not changed after checking with an interference plug gage. This result is encouraging when one considers that the circumferential thermal gradient was 50 to 75 K. Whether thermal stresses resulting from these gradients would affect the long-term creep deformation is open to question. Using telescoping gages and inside micrometers was adequate for measuring the inside diameter because bowing or changes in total indicator reading (TIR) had not occurred. But if changes in TIR or bowing had occurred, special measuring tools would have been necessary. A special tool to measure TIR would certainly have to be developed for longer specimens.

As discussed in the previous section the outside clad measurements indicated strain had occurred. The function of this clad was to prevent  $\text{UO}_2$  loss to the vacuum chamber, to contain the cover gas over the fuel, and to house thermocouples. This outer clad design was not considered to be important in this study because its design would be different for both the reactor test version as well as the thermionic reactor TFE.

### Metallography

The tungsten movement observed in figures 9 and 11 is typical of a tungsten and water reaction since it takes only approximately 20 ppm of water (ref. 8) to start this high-temperature, reversible reaction, which the researchers were unaware of before the start of testing. Although moisture was not measured, it is reasonable to assume that such an amount could have been present considering handling during assembly and the lack of a vacuum bake-out period before high-temperature operation. Metallography does show that gross cracking of the fuel occurred on cooldown, which had been expected. Furthermore, gammagraphs showed that during 50-hour intervals of operation (second specimen) some cracks healed and new ones were formed. After longer operating periods the fuel is still expected to crack since the fuel grain size would increase with operating time (making the structure more brittle). There has been some question as to whether the fuel cover gas would impede fuel redistribution and prevent fuel melting. Fuel melting would occur during heatup when the fuel pulls away from the clad due to differences in the coefficients of thermal expansion. It has been recommended that radial webs in the fuel would prevent fuel melting (ref. 4). The examination of these two specimens showed the fuel had not melted as a result of the fuel pulling away during heatup. However, whether this condition (fuel not melting) will hold when specimens are thermal cycled rapidly (simulating reactor scrams) after densification remains to be proven. This may be a problem since after densification (i. e., after operation periods at design temperature) the fuel is expected to be glass brittle, causing the fuel to frag-

ment on cooldown. It is not known whether the fragmented fuel will mate and heal without localized melting during the next rise in temperature. The results from the gamma-graphs and the metallography show that fuel redistribution occurred during a 240-hour period at design temperature and that fuel melting did not occur. These results imply that radial webs in the fuel as proposed in reference 4 are not necessary. It is possible that densification time would increase with an increase in gap size (between the fuel and inner clad) as well as a decrease in temperature. Thermal conductivity of the fuel appears to have decreased judging from the increase in fuel porosity. Some means of measuring the change in thermal conductivity due to fuel structural change is advisable.

Figures 12 and 13 show the gaps near the heat dams plugging up with fuel. The 0.508-millimeter (0.02-in.) gaps would eventually fill with densified fuel causing the axial heat flow to short circuit through the fuel, rendering these dams useless. It appears that reducing the 0.508-millimeter (0.02-in.) spacing will not solve this problem. The end configuration should be such that fuel can be allowed to fill the spacing without excessive axial heat loss after fuel densification.

#### CONCLUDING REMARKS

This testing program has not demonstrated that the external fuel concept is ready for use in a thermionic reactor. The program did, however, give ample favorable results warranting further development of this concept. The short-term (240-hr) tests reported herein for external fuel configured thermionic emitter specimens showed that:

1. The fuel cracked and the cracks healed when thermally cycled (in the temperature range of thermionic interest) while the inner clad maintained dimensional stability.
2. Fuel melting did not occur during the heatup portion of thermal cycling prior to fuel redistribution.

3. The fuel cover gas does not significantly impede the rate of fuel redistribution.

In general, development effort on this concept is required in the following areas:

- (a) Long-term inpile operation and rapid thermal cycling effects on the inner clad dimensional stability
- (b) Outer clad containment of uranium dioxide and fission gas venting
- (c) Fuel element end design after considering fuel movement, thermal stress, and axial heat losses
- (d) Fuel element length effects on inner clad dimensional stability

Lewis Research Center,  
National Aeronautics and Space Administration,  
Cleveland, Ohio, November 11, 1973,  
503-25.

## REFERENCES

1. Yacobucci, Howard G.: Preliminary Study of a Thermionic Reactor Core Composed of Short-Length Externally Fueled Diodes. NASA TN D-4805, 1968.
2. Mondt, J. F.; and Peelgren, M. L.: External Fuel Thermionic Reactor System. Thermionic Conversion Specialist Conference. IEEE, 1971, pp. 34-40.
3. Schock, A.; Raab, B.; and Giorgio, F.: Design, Fabrication, and Testing of a Full-Length External-Fuel Thermionic Converter. Thermionic Conversion Specialist Conference. IEEE, 1970, pp. 517-532.
4. Davison, Harry W.: The Fuel-Emitter Separation Problem in Externally Fueled Thermionic Diodes. NASA TM X-1812, 1969.
5. Mallerns, F. S., Jr.: Steady State Heat Transfer Program (STHTP). Rep. HW-73668, Hanford Lab., General Electric Co., May 12, 1962.
6. Gluyas, Richard E.: Calculation of Fuel Loss From Vented Nuclear Fuel Elements for Space Power Reactors. NASA TN D-4913, 1968.
7. Conway, J. B.; Hein, R. A.; Fincel, R. M., Jr.; and Losekamp, A. C.: Enthalpy and Thermal Expansion of Several Refractory Metals to 2500<sup>o</sup> C. Rep. GE-TM-64-2-8, General Electric Co., Feb. 1964.
8. Conway, J. B.; Fincel, R. M., Jr.; and Hein, R. A.: The Thermal Expansion and Heat Capacity of UO<sub>2</sub> to 2200<sup>o</sup> C. Trans. ANS, vol. 6, no. 1, June 1963, p. 153.

TABLE I. - SPECIMEN DIMENSIONS

[Both specimens were approximately 3.81 cm (1.50 in.) long.]

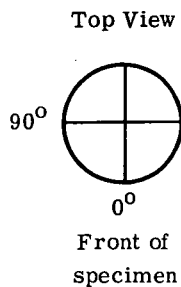
Dimension	Specimen 1 as-built	Specimen 2 as-built	Specimen 2 at operating temperature <sup>a</sup>
Inner clad inside diameter, mm (in.)	12.45 (0.490)	12.45 (0.490)	12.5 (0.494)
Inner clad thickness, mm (in.)	1.52 (0.060)	1.52 (0.060)	1.52 (0.060)
Inner clad fuel radial gap <sup>b</sup> , mm (in.)	0.051 (0.002)	0.051 (0.002)	0.356 (0.014)
Fuel thickness, mm (in.)	3.18 (0.125)	4.57 (0.180)	4.73 (0.186)
Outer clad fuel radial gap <sup>b</sup> , mm (in.)	0.305 (0.012)	0.305 (0.012)	0.076 (0.003)
Outer clad thickness, mm (in.)	2.03 (0.080)	2.03 (0.080)	2.0 (0.80)

<sup>a</sup>1875 K inner clad temperature.

<sup>b</sup>Assuming fuel surfaces concentric with clad surfaces.

TABLE II. - SPECIMEN 2 OUTER CLAD DIMENSIONAL CHANGES

AFTER 240 HOURS



Location	Increase in outer clad outside diameter					
	At 0°			At 90°		
	mm	in.	Percent	mm	in.	Percent
Top blackbody hole	0	0	0	0.028	0.0011	0.095
Middle blackbody hole	.018	.0007	.06	.074	.0029	.25
Bottom blackbody hole	0	0	0	.040	.0016	.14



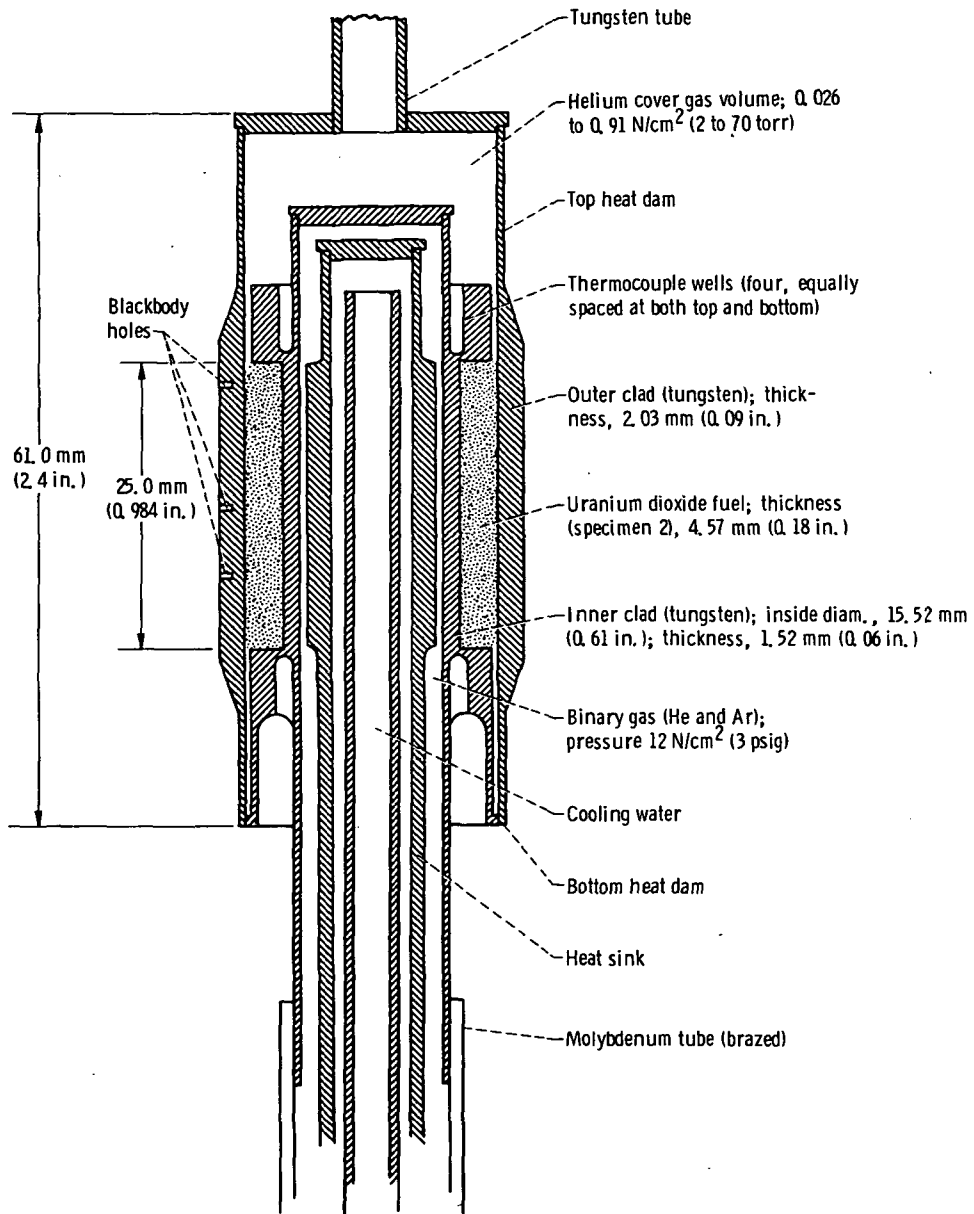
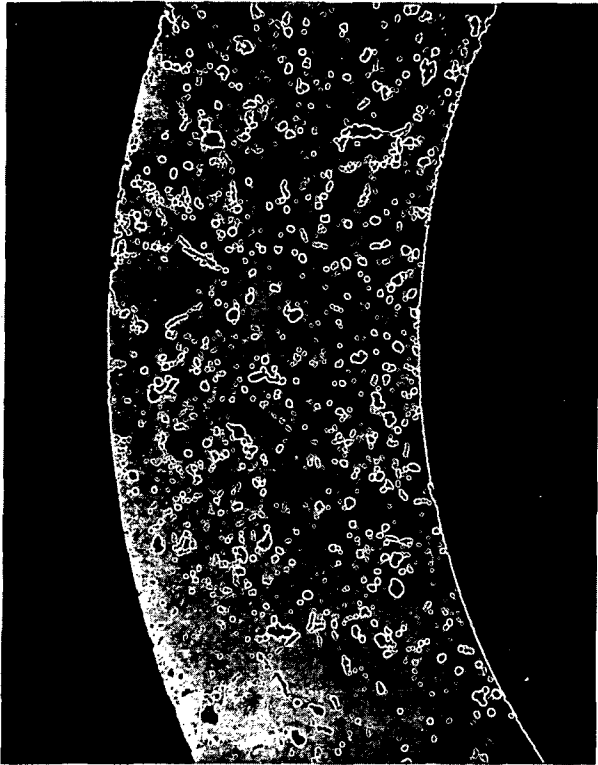
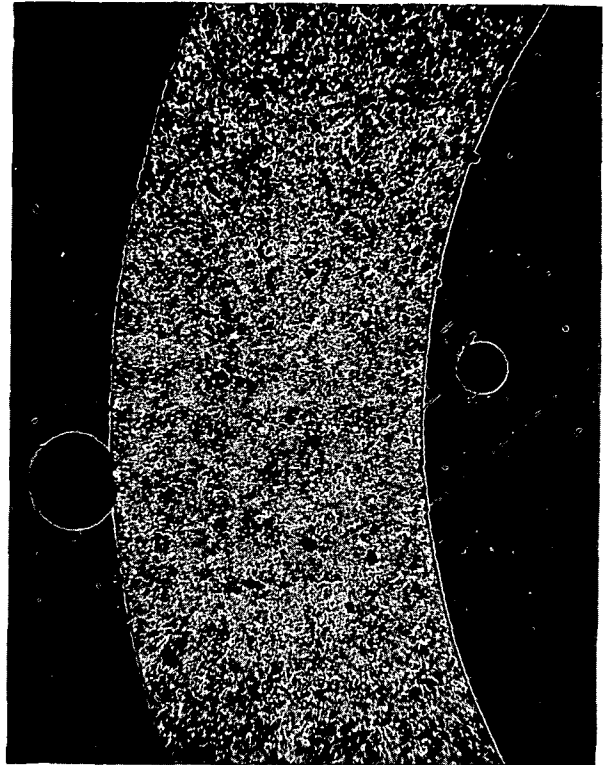


Figure 1 - Schematic of test specimen.



As received; unetched; X15.



As received; etched; X15.

Figure 2. - Microstructure of as received uranium dioxide fuel.

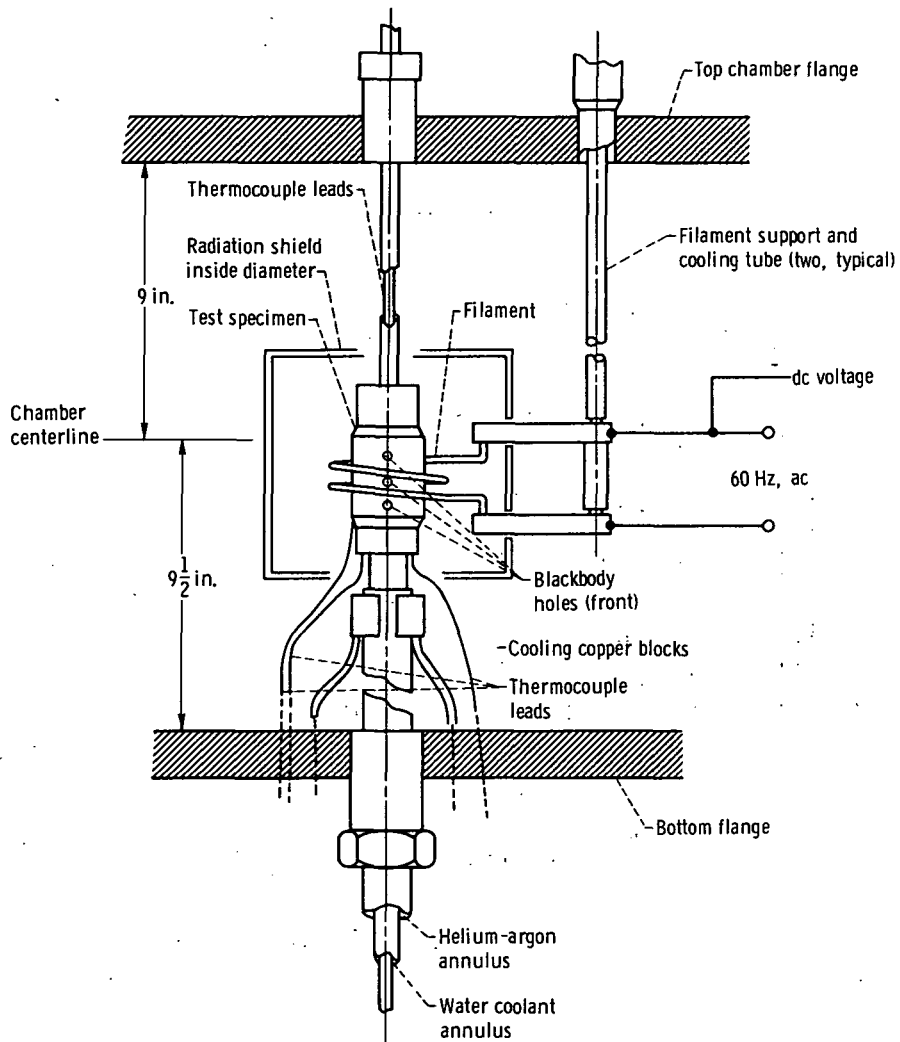


Figure 3. - Test specimen and filament arrangement.

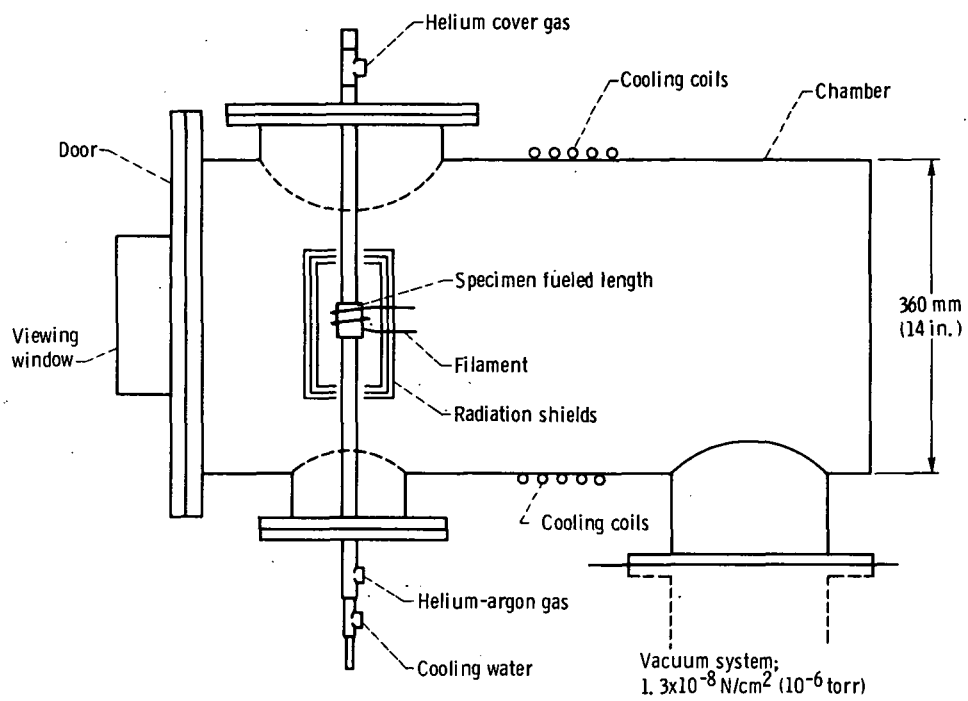


Figure 4. - High-temperature vacuum test chamber and test specimen location.

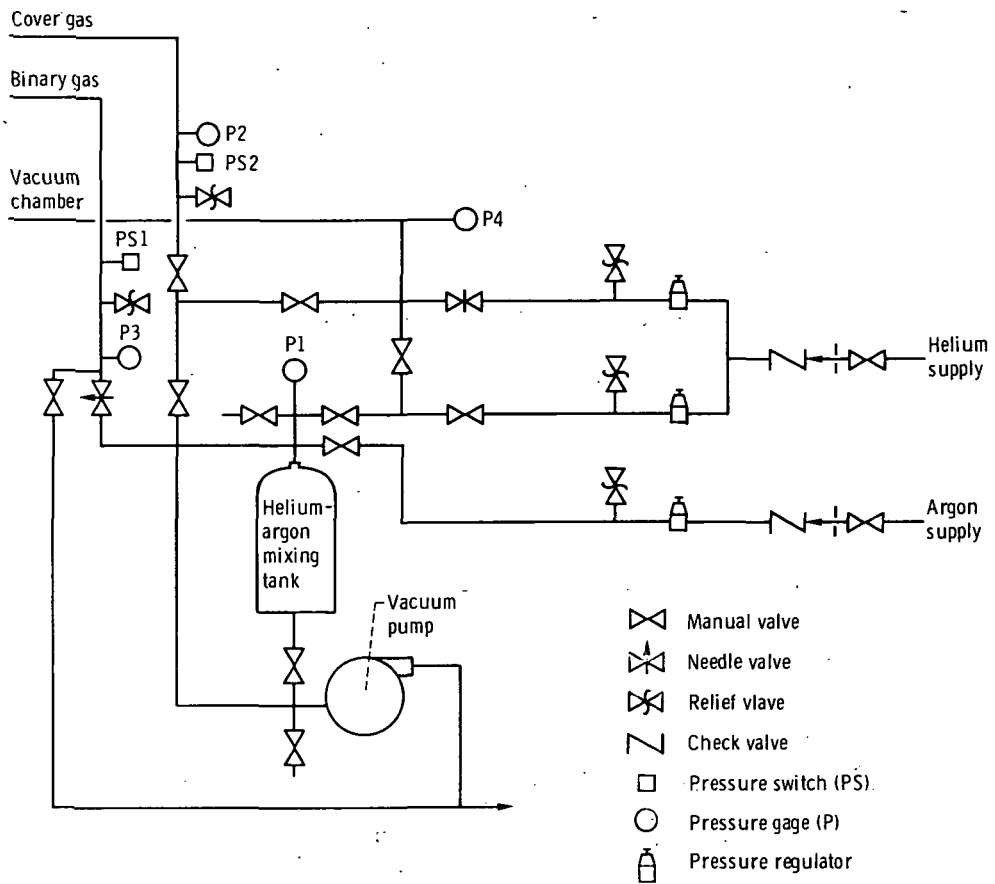


Figure 5. - Gas system schematic

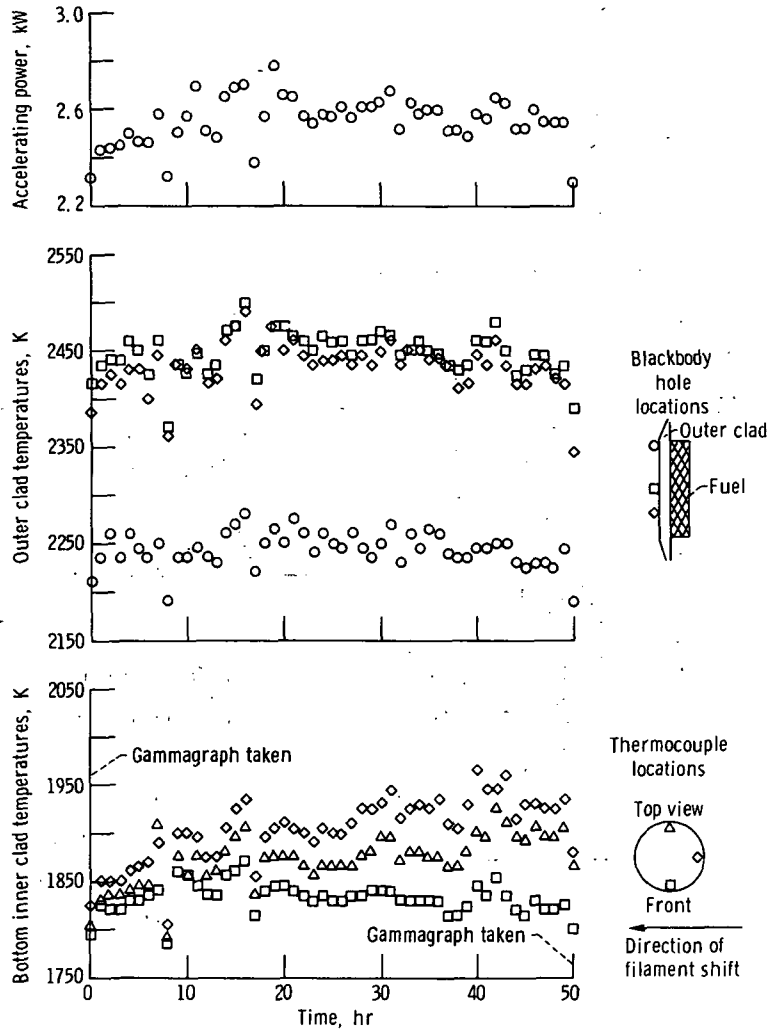


Figure 6. - Specimen 1 operating history.

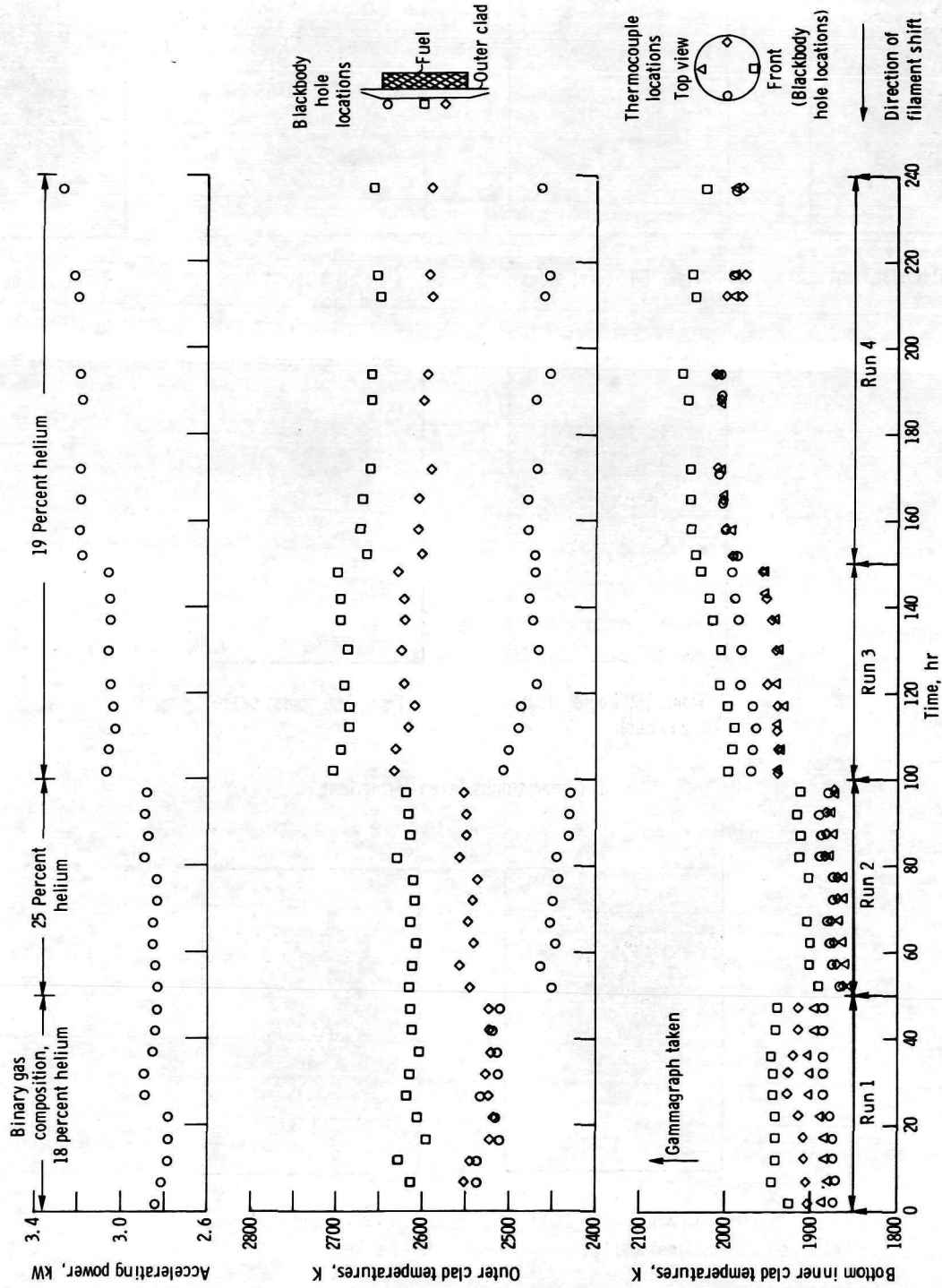
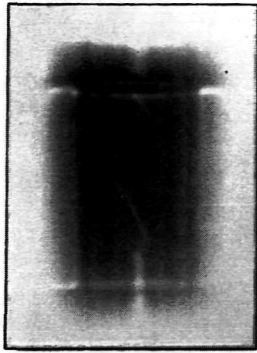
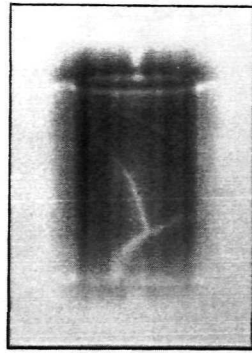


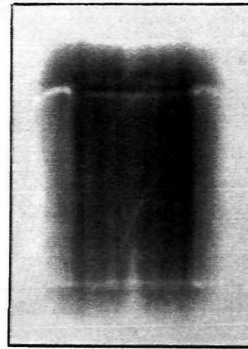
Figure 7. - Specimen 2 operating history.



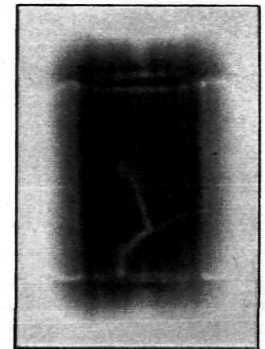
Time, 50 hours; front and back



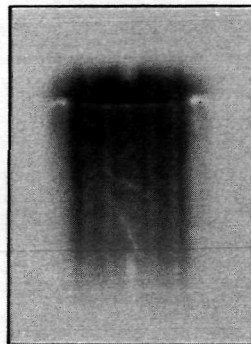
Time, 50 hours; sides



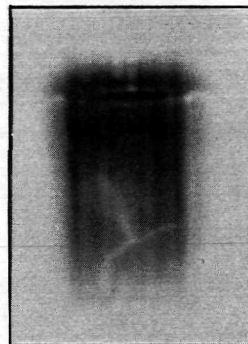
Time, 100 hours; front and back



Time, 100 hours; sides

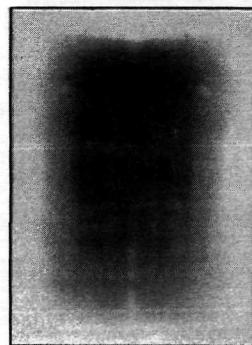


Time, 150 hours; front and back

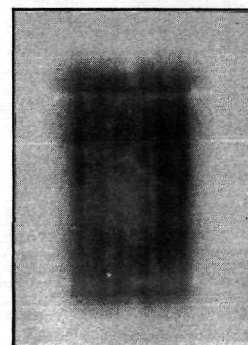


Time, 150 hours; sides

(a) Gammagraphs taken during test.



(b) After test (240 hr); front and back.



(c) After test (240 hr); sides.

Figure 8. - Gammagraphs from specimen 2 taken at various times from start of test.



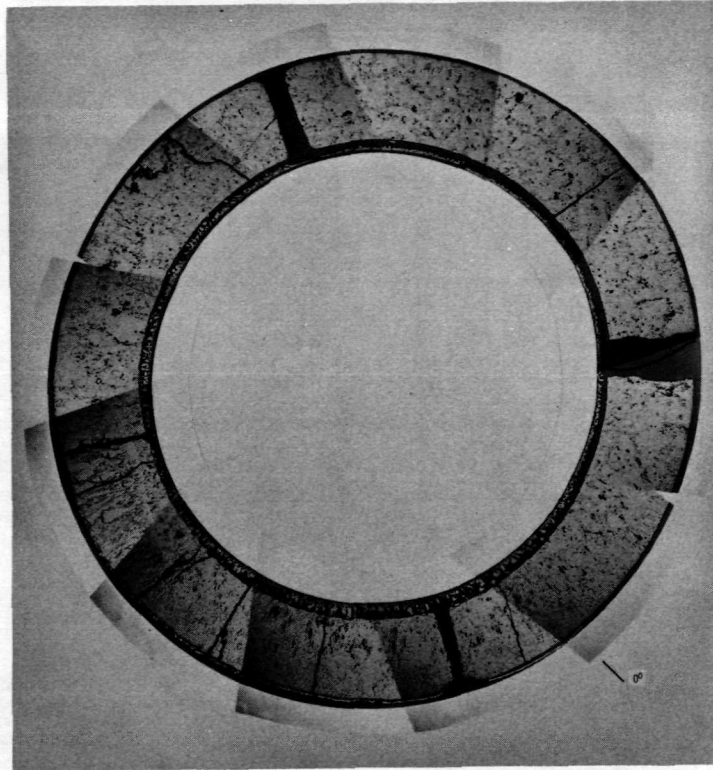


Figure 9. - Specimen 1 after 50 hours and one thermal cycle; unetched, X14.5.

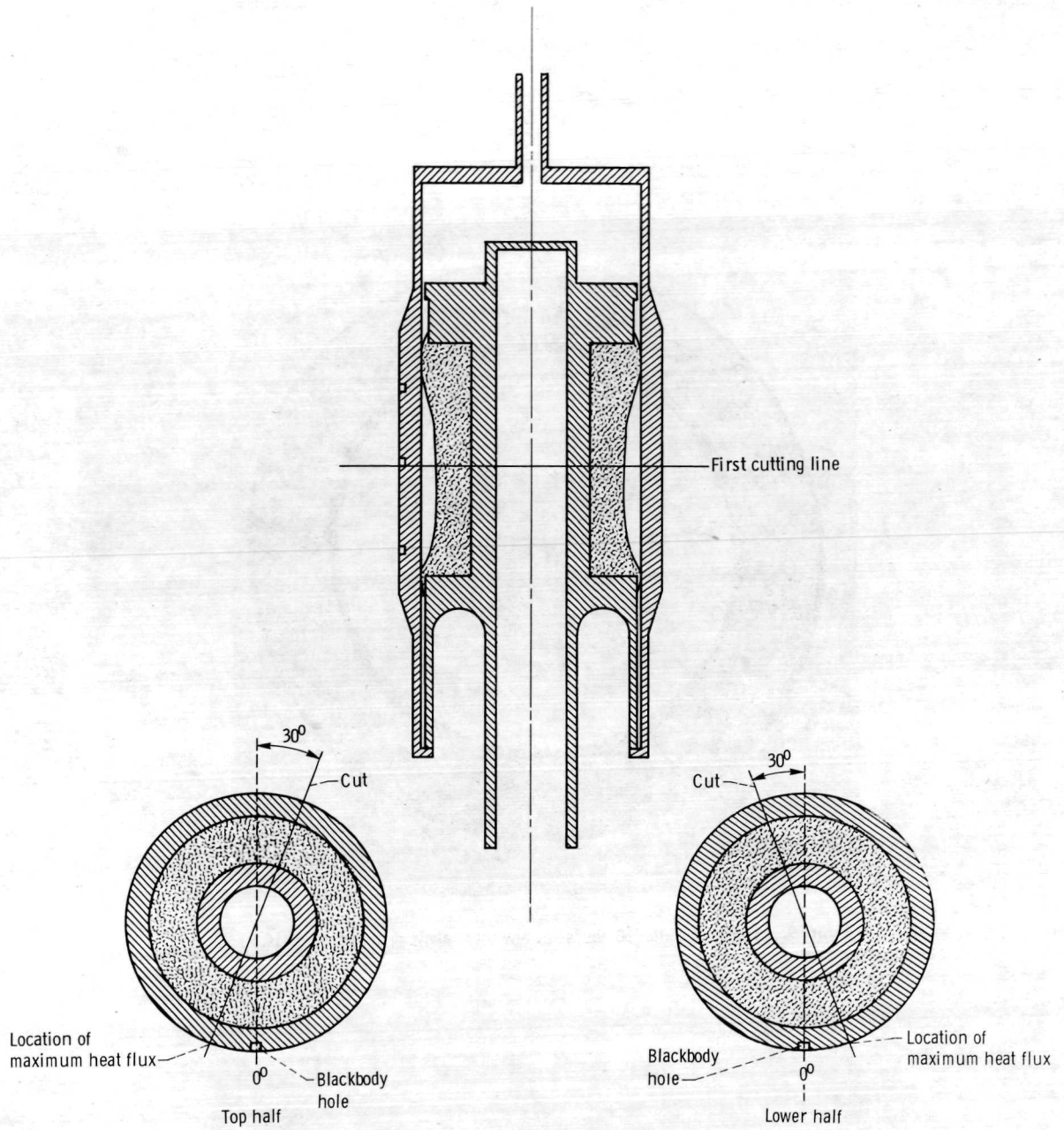


Figure 10. - Specimen 2 cutting diagram.

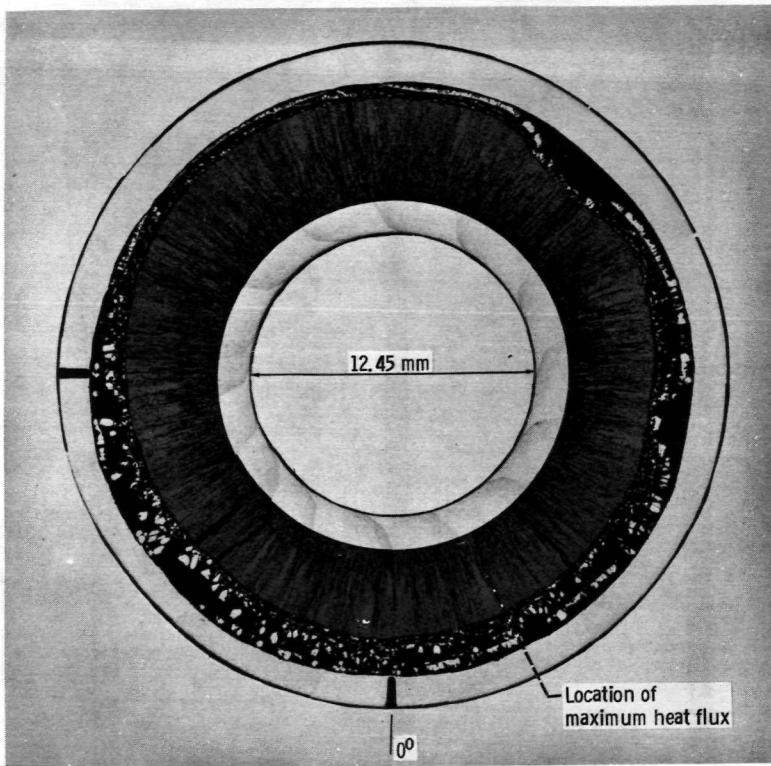


Figure 11. - Top half of specimen 2 after test (240 hr and five thermal cycles); unetched, X12.

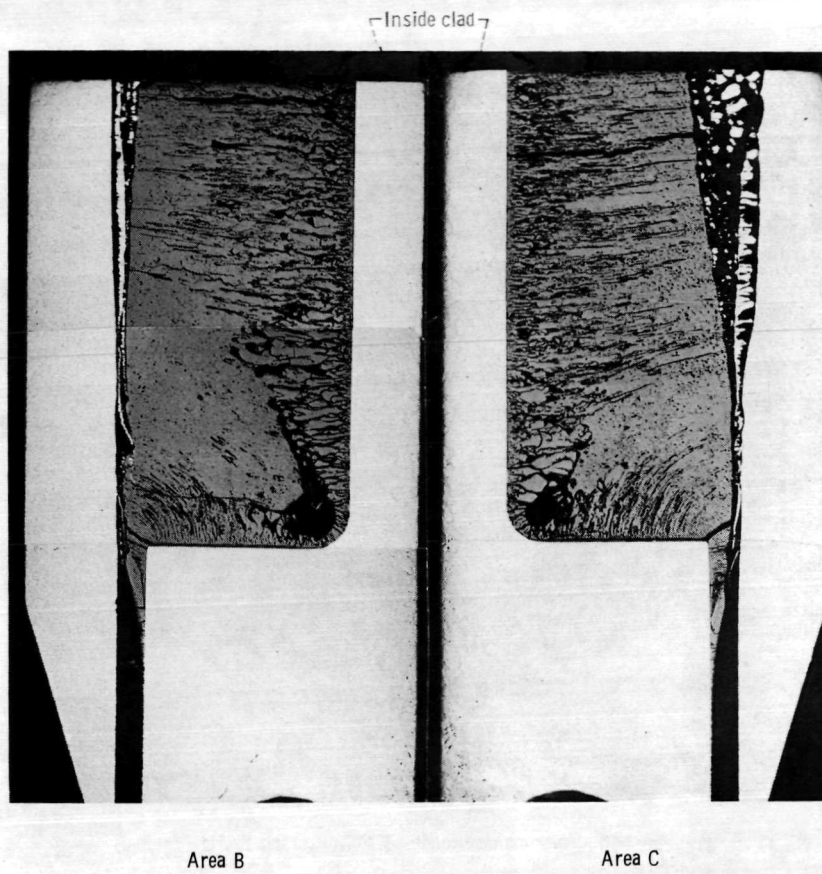


Figure 12. - Bottom half of specimen 2 after test (240 hr and five thermal cycles); unetched. X12.

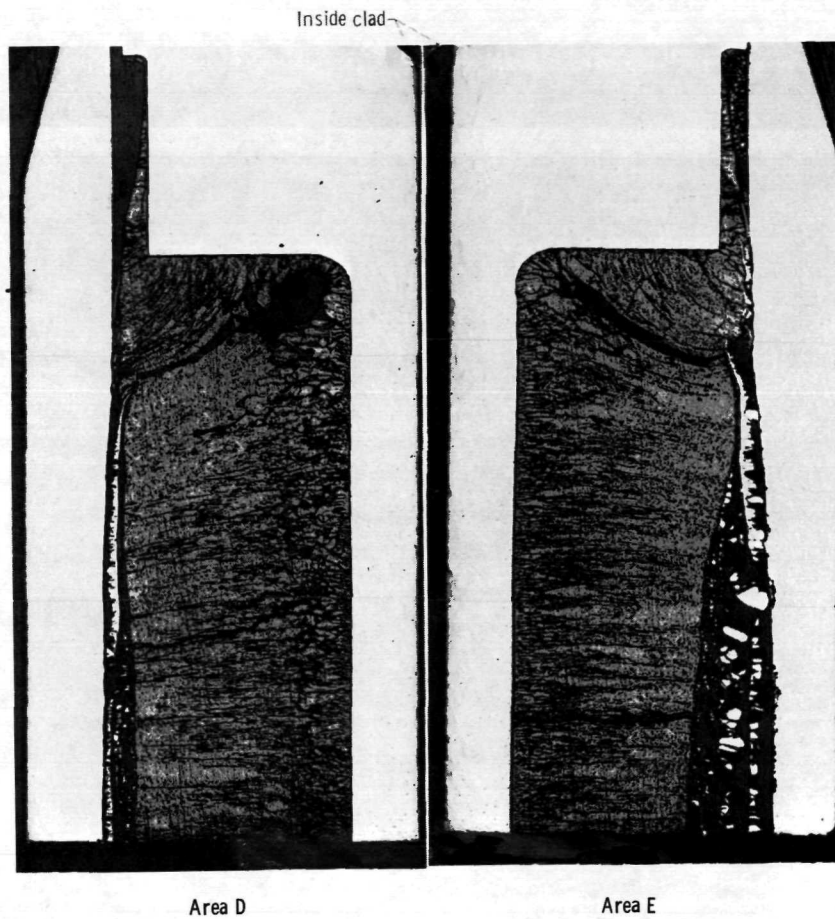


Figure 13. - Top half of specimen 2 after test (240 hr and five thermal cycles); unetched. X12.



POSTMASTER: If Undeliverable (Section 158  
Postal Manual) Do Not Return

*"The aeronautical and space activities of the United States shall be conducted so as to contribute . . . to the expansion of human knowledge of phenomena in the atmosphere and space. The Administration shall provide for the widest practicable and appropriate dissemination of information concerning its activities and the results thereof."*

—NATIONAL AERONAUTICS AND SPACE ACT OF 1958

## NASA SCIENTIFIC AND TECHNICAL PUBLICATIONS

**TECHNICAL REPORTS:** Scientific and technical information considered important, complete, and a lasting contribution to existing knowledge.

**TECHNICAL NOTES:** Information less broad in scope but nevertheless of importance as a contribution to existing knowledge.

**TECHNICAL MEMORANDUMS:** Information receiving limited distribution because of preliminary data, security classification, or other reasons. Also includes conference proceedings with either limited or unlimited distribution.

**CONTRACTOR REPORTS:** Scientific and technical information generated under a NASA contract or grant and considered an important contribution to existing knowledge.

**TECHNICAL TRANSLATIONS:** Information published in a foreign language considered to merit NASA distribution in English.

**SPECIAL PUBLICATIONS:** Information derived from or of value to NASA activities. Publications include final reports of major projects, monographs, data compilations, handbooks, sourcebooks, and special bibliographies.

**TECHNOLOGY UTILIZATION PUBLICATIONS:** Information on technology used by NASA that may be of particular interest in commercial and other non-aerospace applications. Publications include Tech Briefs, Technology Utilization Reports and Technology Surveys.

*Details on the availability of these publications may be obtained from:*

**SCIENTIFIC AND TECHNICAL INFORMATION OFFICE**

**NATIONAL AERONAUTICS AND SPACE ADMINISTRATION**  
Washington, D.C. 20546